Silicon (2017) 9:239–248
DOI 10.1007/s12633-016-9433-9

ORIGINAL PAPER

Thermal, Structural, and Morphological Investigations of Modified Bismuth Silicate Glass-Ceramics

Ahmed H. Hammad[1,2] · A. M. Abdelghany[3] · Hatem A. ElBatal[4]

Received: 1 February 2016 / Accepted: 29 March 2016 / Published online: 24 June 2016

Abstract Glass-ceramics were prepared based on the basic glass composition in mole fraction 0.65 Bi_2O_3 -0.35 SiO_2 with replacements of 0.05 SiO_2 by equivalent of one of the oxides: MoO_3, WO_3, SrO, BaO or CdO. The glass transition temperature of the parent glass is 465 °C which is observed to decrease when doped with Mo, W, Sr, Ba, or Cd oxides. A eulytite phase is formed through controlled crystallization of the parent glass-ceramic and the samples doped with Mo or W, while a $Bi_2O_2SiO_3$ phase is detected for the samples doped with Sr and Cd. Orthorhombic bismuth silicate crystals were observed only in the sample doped with Ba. SEM images show that all samples have elongated particles with few rectangular or spherical crystals. BiO_6 and BiO_3 units are assumed to be formed in all samples within the characteristic IR silicate absorption bands.

✉ Ahmed H. Hammad
ahmed_hammad81@ymail.com; ahosny2005@gmail.com; ah.hammad@nrc.sci.eg

[1] Center of Nanotechnology, King Abdulaziz University, Jeddah, Saudi Arabia

[2] Electron Microscope and Thin Films Department, Physics Division, National Research Centre, 33 El-Behouth St., Dokki, 12622, Cairo, Egypt

[3] Spectroscopy Department, Physics Division, National Research Centre, 33 El-Behouth St., Dokki, 12311, Cairo, Egypt

[4] Glass Department, National Research Centre, 33 El-Behouth St., Dokki, 12311, Cairo, Egypt

Keywords Thermal expansion · Electron microscopy · FTIR spectroscopy · Glass-ceramics · Bismuth silicate · X-ray diffraction

1 Introduction

Unconventional and heavy metal oxide glasses based on Bi_2O_3 have interesting applications as non-linear optical materials due to their novel high refractive index which is useful for ultrafast optical switches, and optoelectronic devices [1–4]. Moreover, glasses based on PbO and Bi_2O_3 are essentially suitable for photonic crystal fiber and micro-optical element development [5]. Bismuth–silicate glasses have been favorably used as low loss optical fibers, infrared transmitting materials due to their long infrared cut-off wavelengths [6, 7]. Several studies were made on the constitution of bismuth silicate glasses by infrared, and Raman spectroscopy [8–11]. It have been proved that Bi^{3+} ions can act as a network modifier and/or as a network former in the form of $[BiO_n]$ (n = 3, or 6) pyramidal units and the ratio of each unit is strongly dependent on the glass composition.

When glasses are thermally heat treated by a two-stage process; i.e. first near the glass transition temperature to cause a nucleation process followed by further heating the glasses to higher temperature which is called the crystallization process, glasses are converted to their corresponding glass-ceramic materials. Glass-ceramics have valuable advantages rather than conventional glasses and ceramics [12, 13]. Glass-ceramics can be defined as combining the properties of glasses and ceramics. Hence, it is important to investigate the behavior of the inorganic phases on the physical-chemistry properties of the glass-ceramic materials as well as the thermodynamic and kinetic parameters [14]. Water molecules can exist as traces in most inorganic

materials like glass, ceramics, and glass-ceramics which are assumed to have some effects on the physical, chemical, mechanical and technological properties [15, 16].

Gerth and Rüssel [17] successfully deposited the ferroelectric Bi_3TiNbO_9 as the main phase from $Bi_2O_3/TiO_2/Nb_2O_5/B_2O_3/SiO_2$ glasses by heat-treating the glasses at 700 °C/ 2 h for borate containing glass and 860 °C/ 2 h for silicate glass. Other phases were detected from X-ray diffraction (XRD) such as $Bi_2Ti_2O_7$, $Bi_7Ti_4NbO_{21}$, $BiNbO_4$ and $Bi_5Nb_3O_{15}$ phases. Also, they showed the ferroelectric crystals were separated within the glassy phase in borate glass-ceramics while those crystals were interconnected in silicate glass-ceramics.

Abo-Naf et al. [18] studied SiO_2-PbO-Bi_2O_3 glasses and their corresponding glass-ceramics. They reported that $SiPbBi_2O_6$ glass nano-composites comprising bismuth oxide nano-crystallites were obtained through the zero nucleation rate with a diffusion controlled growth at the crystallization temperature (T_c) for 10 h. Nano-crystallite sizes varied from 15 to 170 nm depending on the parent glass composition.

Transparent crystallized glasses containing bismuth like $LaBGeO_5$, $SrBi_2Ta_2O_9$ and $Ba_2TiGe_2O_8$, which are applicable as optical non-linear and ferroelectric crystals, have been fabricated by several authors [19–21].

Moreover, transparent glass-ceramics have been obtained from a sodium lead bismuth silicate glass system containing chromium oxide as a dopant [22]. The host glass ceramic has a major phase of sodium silicate and two minor phases of lead silicate and bismuth oxide. The presence of Cr_2O_3 in the host glass is assumed to provide the additional crystal phases of $NaCrO_2$, $Na_2Cr_2O_7$ and $Pb(CrO_4)$. The spectroscopic studies of such glass ceramics have proved that the higher ratio of the chromium dopant is mostly existing in the trivalent Cr^{3+} state and occupies a octahedral position in the glass ceramic matrix which is suitable for lasing action.

Fu et al. [23] investigated the glass system of samarium doped lithium yttrium aluminum silicate (LYAS) for optoelctronic devices. They found that at the high heat treatment regime, an orientational crystallization observed. Visible transmission emissions studies of Sm^{3+} indicated that Sm^{3+} ions are present as micro-crystals formed in the glass ceramics. Furthermore, when bismuth silicate glasses are doped with Nd^{3+} ions, it improves the thermal stability and is improvement against crystallization and these glasses have great applicability for 1.06 μm laser application [24].

Cheng et al. [19] detected crystalline phases of $Bi_6B_{10}O_{24}$, $Bi_4B_2O_9$ and $BiBO_3$ obtained from the Bi_2O_3-B_2O_3 glass system. $BiBO_3$ phase has been obtained when the bismuth content is over 45 mol%. Moreover this phase has a technological application in non-linear optical materials [25, 26].

The main objective of this work is to prepare binary bismuth silicate of the composition 65 mol% Bi_2O_3 – 35 mol% SiO_2 together with samples containing 5 % of any of the oxides (MoO_3, WO_3, SrO, BaO or CdO) replacing equivalent SiO_2. The prepared glasses have been investigated by collective Fourier transform infrared and thermal expansion measurements. The same measurements have been repeated for derived glass-ceramics prepared by controlled two-step thermal treatments with X-ray diffraction and scanning electron microscopy to find the crystalline phases separated during heat-treatment, their morphological texture and their constitutional presence within the silicate network.

2 Experimental Details

2.1 Glass Syntheses

The glasses were prepared from chemically pure reagents of pulverized quartz (Fluka, Germany) with Bi_2O_3 (Rasayan Laboratory, India), MoO_3 and WO_3 (Rasayan Laboratory, India) added as received while SrO, BaO and CdO were used in their carbonate form and supplied also by Rasayan Laboratory, India with nominal composition shown in Table 1.

Glass monoliths of the base composition or of the doped compositions described before were mixed in Pt crucibles placed in a high temperature electrical furnace (Vecstar, UK) at about 1200 ±10 °C for a suitable interval of time (about 2h) depending on the glass composition under ordinary atmospheric conditions. During melting, the crucibles were occasionally rotated to achieve acceptable mixing and homogeneity. The melts were poured into preheated stainless steel molds of the required dimensions and the samples were immediately transferred to a muffle furnace for annealing adjusted at about 400 °C. The annealing muffle was maintained at this temperature for 1h and then switched off to cool gradually to room temperature at a rate of nearly 30 °C/ h.

Table 1 Glass composition in mol%

Sample	Bi_2O_3	SiO_2	MoO_3	WO_3	SrO	BaO	CdO
BiSi	65	35	-	-	-	-	-
BiSiMo	65	30	5	-	-	-	-
BiSiW	65	30	-	5	-	-	-
BiSiSr	65	30	-	-	5	-	-
BiSiBa	65	30	-	-	-	5	-
BiSiCd	65	30	-	-	-	-	5

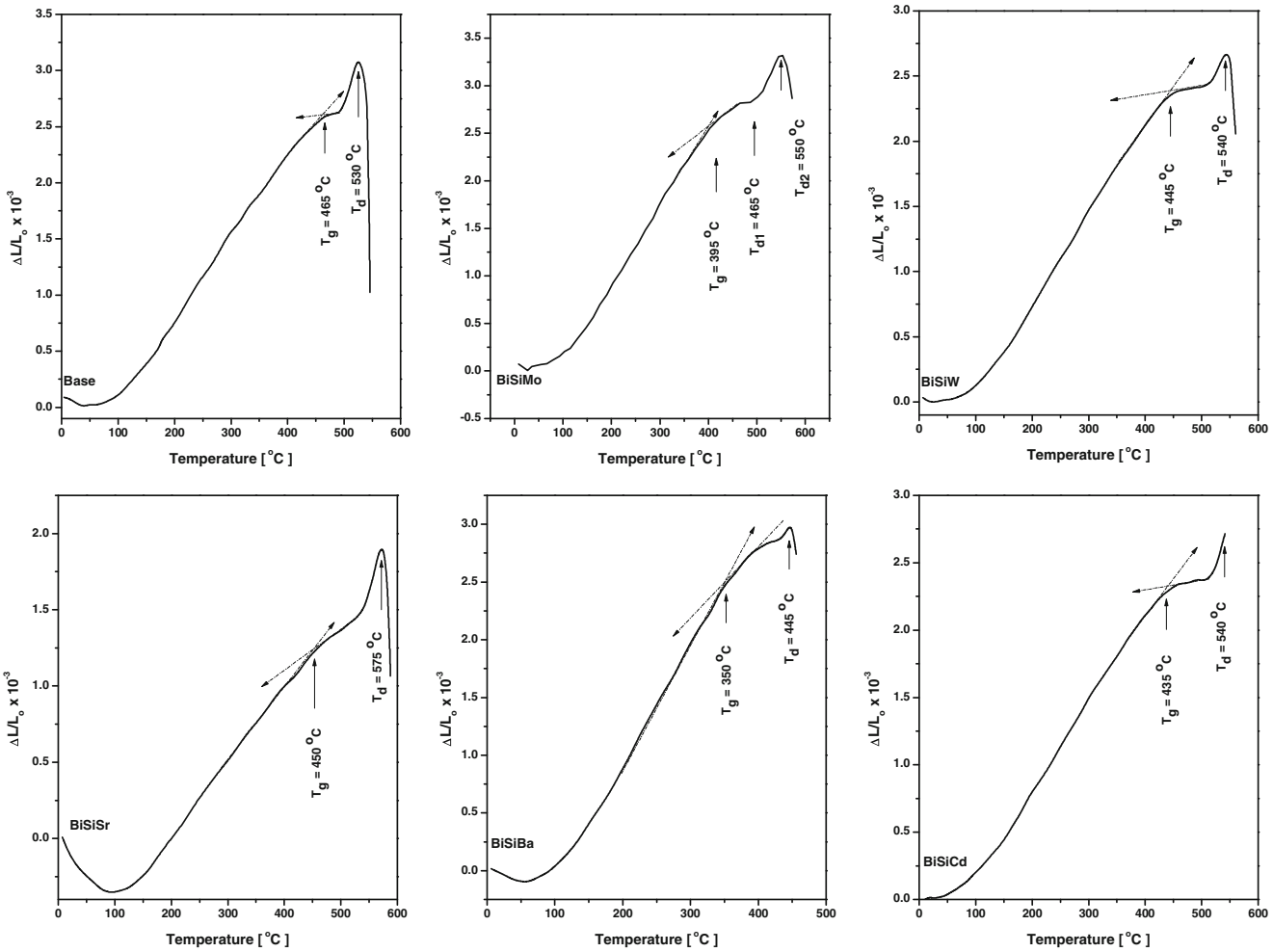

Fig. 1 The dimensional change in length ($\Delta L/L_o$) vs. temperature for the glass samples

2.2 Thermal Expansion Measurements

Thermal expansion behavior of the glasses was measured using a computerized dilatometer (type NETZSCH, 402PC). All measurements were made in the temperature range from room temperature up to the dilatometric softening temperature (T_d) with a heating rate of 5 °C /min. The glass samples with equal dimensions (1 ×3 cm) were used and at least two measurements were made for each glass composition and the experimental results were found to be reproducible (±0.01 %).

2.3 Preparation of Glass-Ceramic Derivatives

In order to obtain glass-ceramic materials from the prepared parent glasses, an important heat treatment with two steps is necessary; first at the glass transition temperature (T_g) which is assumed to create the crystal nuclei and second at the softening temperature to grow the nuclei to full crystals. In the present work, the glasses were heat treated according to the temperature data obtained from the dilatometer for 3h holding for each step.

2.4 Infrared Absorption Measurements

The infrared absorption spectra of bismuth silicate glass-ceramics containing MoO_3, WO_3, SrO, BaO, and CdO were measured at room temperature in the wavenumber range 4000-400 cm^{-1} by a Fourier Transform computerized infrared spectrometer type (JASCO-FTIR-300E). The samples were investigated as fine powders which were mixed with KBr in the ratio 1:100 mg glass powder to KBr respectively. The weighed mixture was then subjected to a pressure of 5 ton/cm^2 in order to produce clear homogenous discs. The IR spectra were measured immediately after discs preparation.

The deconvolution process is done for the modified base bismuth silicate glass-ceramic samples by the Peak Fit program (Jandel Scientific Peak Fit, copyright©1990 AISN Software) in order to define hidden peaks. The dark current

Table 2 Glass transition temperature; T_g, dilatometric softening temperature; T_d, temperature difference; ΔT, and thermal expansion coefficient; α for bismuth silicate glasses

Glass symbol	T_g[°C]	T_d[°C]	$\Delta T = T_d - T_g$[°C]	$a \times 10^{-6}(°C)^{-1}$	
				100 °C	300 °C
Base	465	530	65	1.064	5.176
BiSiMo	395, 465	550	155, 85	1.919	5.825
BiSiW	445	540	95	1.217	4.893
BiSiSr	450	575	125	-3.48	1.685
BiSiBa	350	445	95	0.406	6.566
BiSiCd	435	540	105	2.032	4.980

noises and background were corrected by two point base line corrections. After successive trials were done, the fitted data were recorded by using spectral Gaussian peaks as described elsewhere [27–29].

2.5 X-ray Diffraction Analysis

The crystalline phases which are obtained during the controlled thermal heat treatment were studied by X-ray diffraction using a Bruker AXS diffractometer (D8-ADVANCE) with Cu-Kα radiation, operating at 40 kV and 10 mA. The diffraction data were recorded for 2θ values between 4° and 70° and the scanning rate was 10°/min.

2.6 Scanning Electron Microscope Investigation

The surface morphology of the corresponding glass-ceramic samples was studied to demonstrate the differences between the samples due to the different additives. The samples were fractured and immersed in 0.05 % dilute HF solution for 40 s. After that, the samples were studied by SEM (type JXA 840A Electron Probe Micro-analyzer operated at 30 KV).

3 Results and Discussion

3.1 Thermal Properties

Thermal behavior of the prepared glasses is necessary to determine the glass transition temperature (T_g) and the softening temperature (T_d). Figure 1 shows the dimensional change of length ($\Delta L/L_o$) as a function in temperature for all the glass samples. The glass transition temperature can be determined at the point of the intersection of the corresponding regression dashed lines while the softening temperature is taken from the exothermic peak. Table 2 reports the values of T_g, T_d, the change between these temperatures ($\Delta T = T_d - T_g$) and the thermal expansion coefficient α.

Thermal parameters such as glass transition temperature (T_g) and dilatometric softening temperature (T_d) are important data and are useful to characterize and describe glasses. The glass transition temperature (or the glass transformation temperature) denotes the onset of viscoelastic behavior, whereas the dilatometric softening temperature shows the onset of flow under a modest load. Each of these properties is strongly dependent on the glass composition. As clearly seen in Fig. 1 the glass transition temperature of the parent Bi_2O_3-SiO_2 glass is 465 °C which decreases when the parent glass is doped with MoO_3, WO_3, SrO, BaO, and CdO. The BiSiBa glass has the lowest glass transition temperature value around 350 °C and the lowest dilatometric softening temperature at 445 °C, whereas the BiSiMo sample exhibits two glass transition temperatures at about 395 and 465 °C. the highest dilatometric softening temperature is also observed in the BiSiSr sample with a peak at 575 °C.

It is known that the addition of modifier ions to silica glass fills the interstices, which prevents the bond bending and hence the thermal expansion coefficient will then increase [13]. This behavior is clearly observed in Table 2 when glasses were doped with some oxides except for the BiSiSr sample.

A negative thermal expansion coefficient is observed at 100 °C for the BiSiSr glass. This is due to the ability of

Table 3 The crystalline phases obtained from X-ray diffraction patterns

Glass symbol	Crystalline phase	JCPDS card number
BiSi	BiO	(27-0054)
	Eulytite	(76-1726)
BiSiMo	Eulytite	(76-1726)
BiSiW	Eulytite	(76-1726)
BiSiBa	BaO	(22-1056), (01-0746)
	Bi_2SiO_5	(36-0287)
BiSiSr	Bi_2O_3	(74-1375)
$Bi_2O_2SiO_3$	(75-1483)	
BiSiCd	$Bi_2O_2SiO_3$	(75-1483)

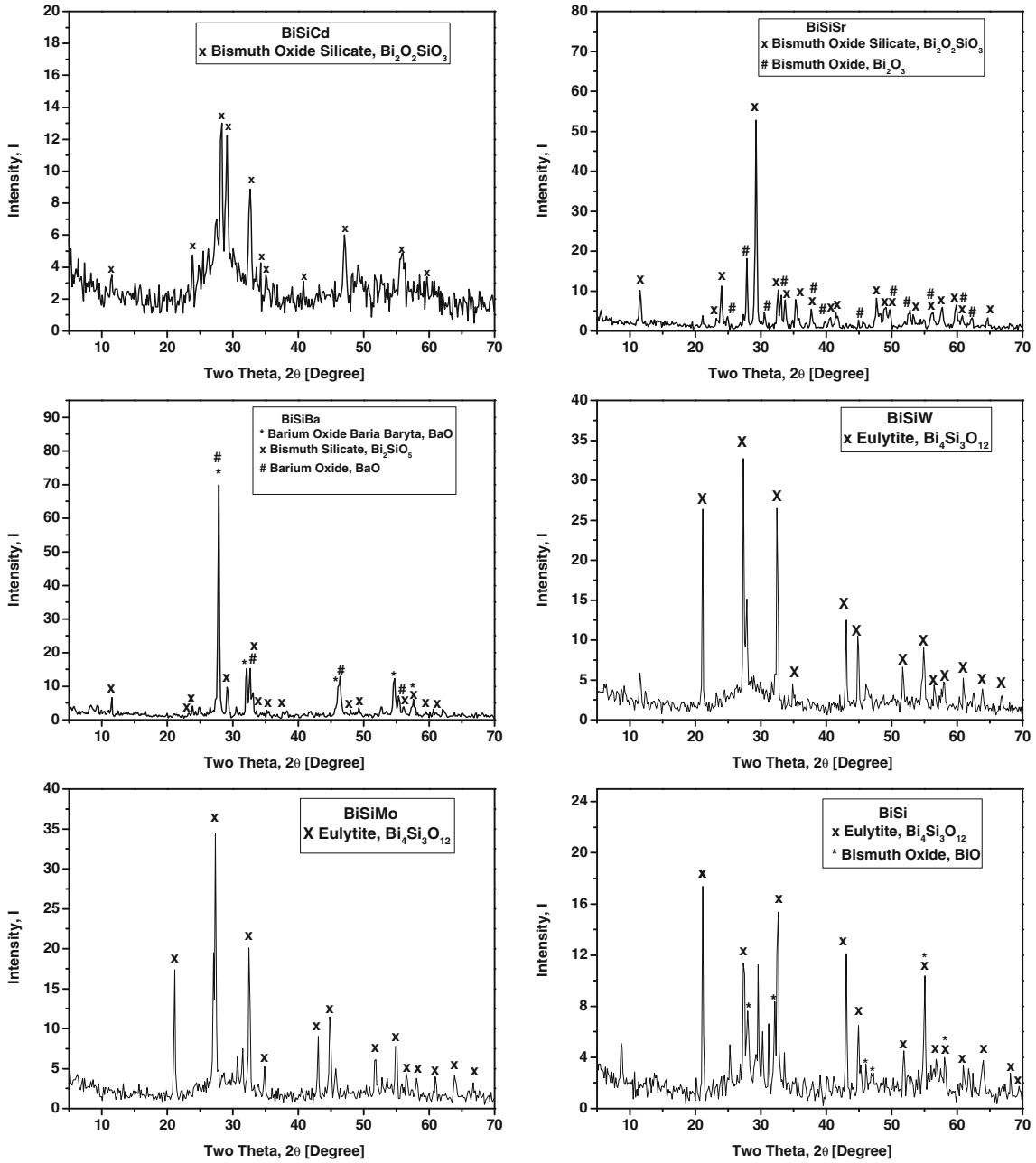

Fig. 2 X-ray diffraction patterns for the base bismuth silicate glass-ceramics and samples containing MoO_3 WO_3, BaO, SrO, and CdO

the network to absorb lattice expansion through bending of bonds into the empty interstices of the structure [13]. Moreover, the glasses doped with alkaline earth oxides like SrO and BaO have lower thermal expansion values than other glasses and the same previous interpretation can be taken into account.

From the dilatometer curves, if only one T_g is detected, it will be that of the less viscous phase. If two transition temperatures are observed, it means that the lower T_g value is for the less viscous phase, while the high T_g value is for the more viscous phase. The glass sample BiSiMo exhibits two glass transformation temperatures. So, it can be deduced that this sample contains two phases due to the interaction of Mo ions with two different glass network formers Bi_2O_3 and SiO_2.

It is worth mentioning that the difference between the glass transition temperature (T_g) and the dilatometric softening temperature (T_d) is much greater than 50 K for all glass samples, so the samples probably have phase separation with a continuous higher viscosity phase [13].

3.2 X-ray Diffraction Analysis

Figure 2 shows the formation of different crystalline phases during the thermal annealing processes. Eulytite ($Bi_4Si_3O_{12}$), bismuth oxide (BiO), barium oxide (BaO), bismuth silicate (Bi_2SiO_5), bismuth oxide (Bi_2O_3) and bismuth oxide silicate ($Bi_2O_2SiO_3$) phases were obtained from the crystallization of glass samples. Table 3 describes the crystalline phases and their corresponding JCPDS cards number.

3.2.1 Formation of Eulytite Phase in Bismuth Silicate Glass-Ceramics

The X-ray diffraction pattern of the BiSi glass-ceramic sample is shown in Fig. 2. It shows the formation of cubic eulytite ($Bi_4Si_3O_{12}$) and rhombohedral bismuth oxide (BiO) phases. The intensity ratio of both phases is 50 %, while the S-Q BiO phase is 91.2 % and for eulytite is 8.8 %. Hence, the major phase in the base BiSi glass-ceramic is BiO phase rather than $Bi_4Si_3O_{12}$ phase.

On the other hand, Fig. 2 shows the BiSi samples doped with heavy transition metal oxides such as MoO_3 and WO_3 (BiSiMo, BiSiW). It is observed that the eulytite phase is the only essential phase and there is no detection of BiO crystals in theses glass-ceramic systems. So, the presence of Mo or W as dopants in the host BiSi glass-ceramics enforces the growth of eulytite phase rather than the base BiSi glass. Furthermore, the base glass composition comprises of 65 % Bi_2O_3 and 35 % SiO_2 which logically makes the growth of BiO crystals as the primary phase. Also, the intensity of eulytite phase is 75 % in BiSiW, greater than the intensity in BiSiMo (68.75 %).

3.2.2 Formation of BaO and Bi_2SiO_5 Phases in Bismuth Silicate Glass-Ceramics

When glass-ceramics of BiSi were doped with BaO, three phases were detected from the X-ray diffraction pattern as

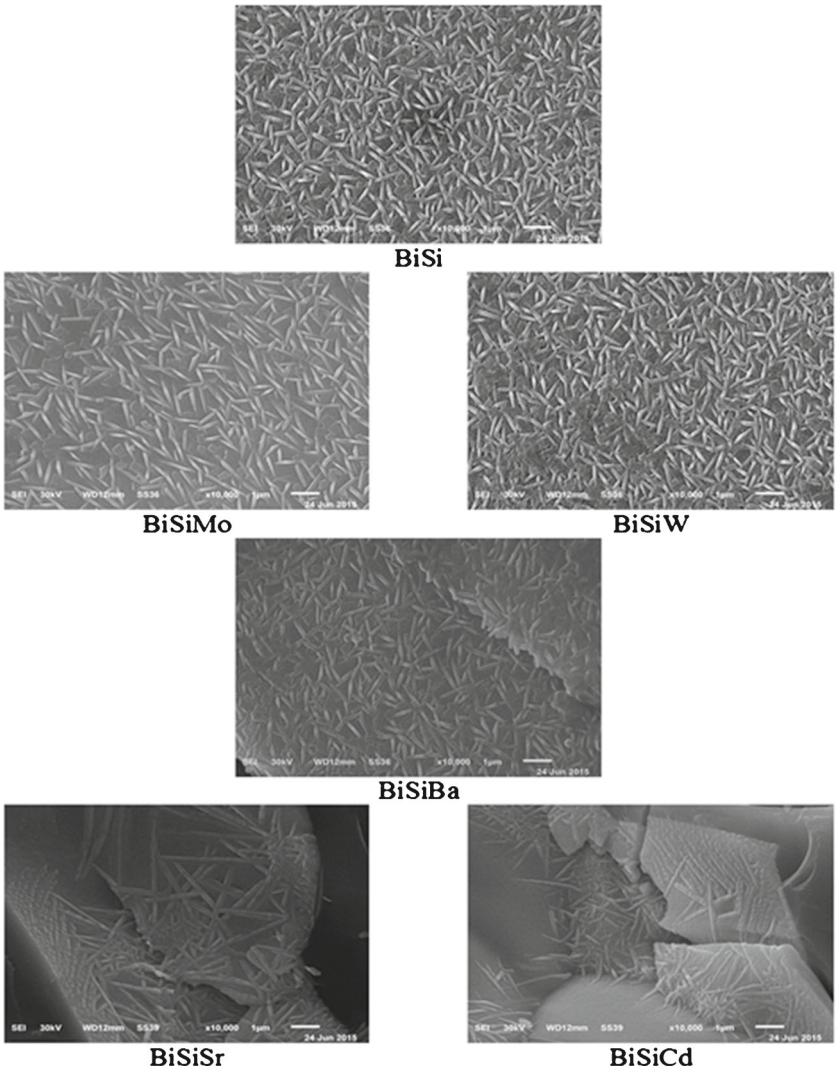

Fig. 3 Morphological structures for the bismuth silicate glass-ceramics

shown in Fig. 2. Orthorhombic bismuth silicate Bi_2SiO_5, cubic barium oxide baria baryta BaO, and cubic barium oxide phases were determined by XRD analysis with S-Q 25.8 %, 54.8 %, and 19.4 %, respectively. So, the barium oxide baria baryta phase represents the major phase in such glass-ceramic systems. The total S-Q of barium oxide is 74.2 % which means that the formation of BaO crystals is easier than the formation of Bi_2SiO_5 crystals. This may be because the activation energy for the formation of BaO is smaller than the activation energy for the formation of Bi_2SiO_5 phase.

3.2.3 Formation of $Bi_2O_2SiO_3$ Crystal

Orthorhombic bismuth oxide silicate ($Bi_2O_2SiO_3$) phase is formed during the conversion of BiSiSr and BiSiCd glasses to glass-ceramics as clearly observed in Fig. 2. In the BiSiSr glass-ceramics, there is another cubic Bi_2O_3 phase formed besides the $Bi_2O_2SiO_3$ phase. The S-Q of Bi_2O_3 is greater than $Bi_2O_2SiO_3$ (56 % and 44 % respectively), but the intensity of the peaks have the same ratio (50 %). When SrO is replaced with CdO, the Bi_2O_3 phase disappears and the $Bi_2O_2SiO_3$ phase is the main and unique phase. This behavior may be attributed to the presence of CdO dopant in the BiSi glass which reduces the Bi_2O_3 phase and strengthens the bismuth oxide silicate phase.

Finally, it can be said that the dopants in the glass-ceramic matrices play a key role in depositing the crystalline phases and enhancing the main phase as previously described. WO_3 and CdO can be used as nucleation agents for the formation of eulytite ($Bi_4Si_3O_{12}$) and bismuth oxide silicate ($Bi_2O_2SiO_3$) phases, respectively.

3.3 Morphological Investigations

Bismuth silicate glass-ceramic samples were surface scanned by SEM as shown in Fig. 3. All samples have

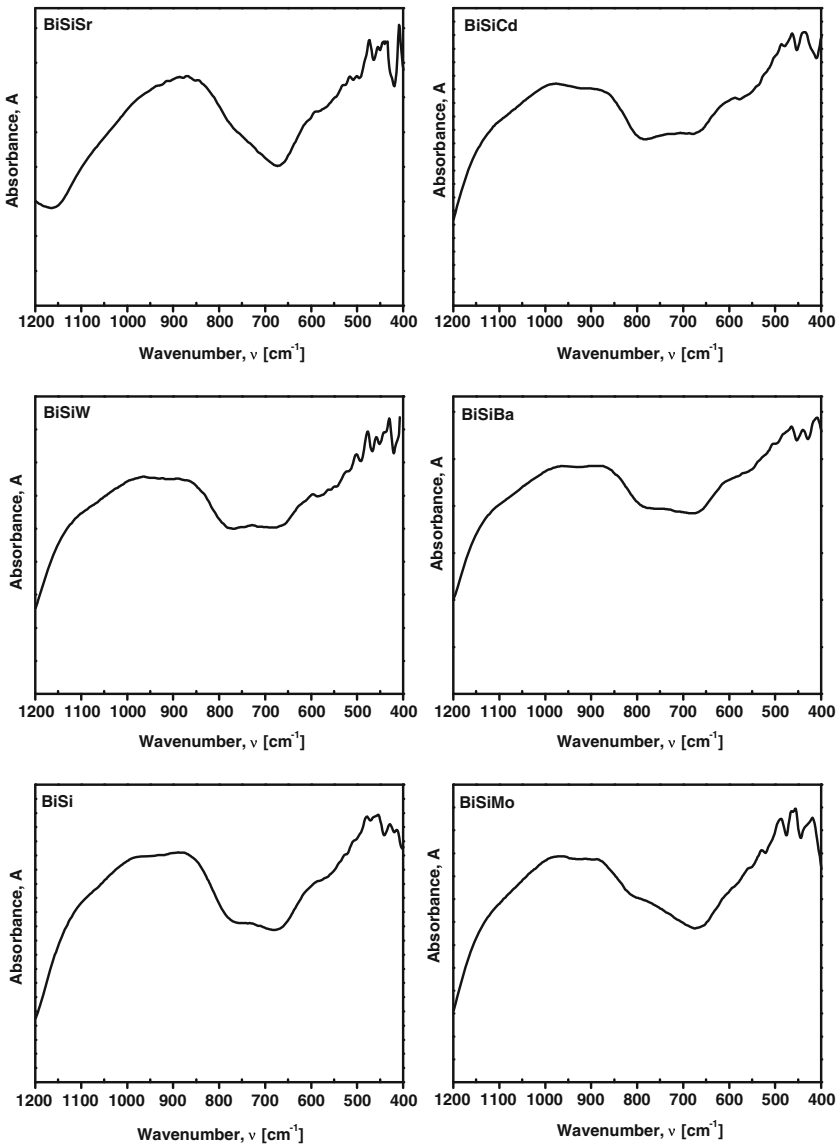

Fig. 4 **a** Infrared absorption spectra in the range 1200-400 cm^{-1}. **b** Infrared absorption spectra in the range 4000-1200 cm^{-1}

Fig. 4 continued

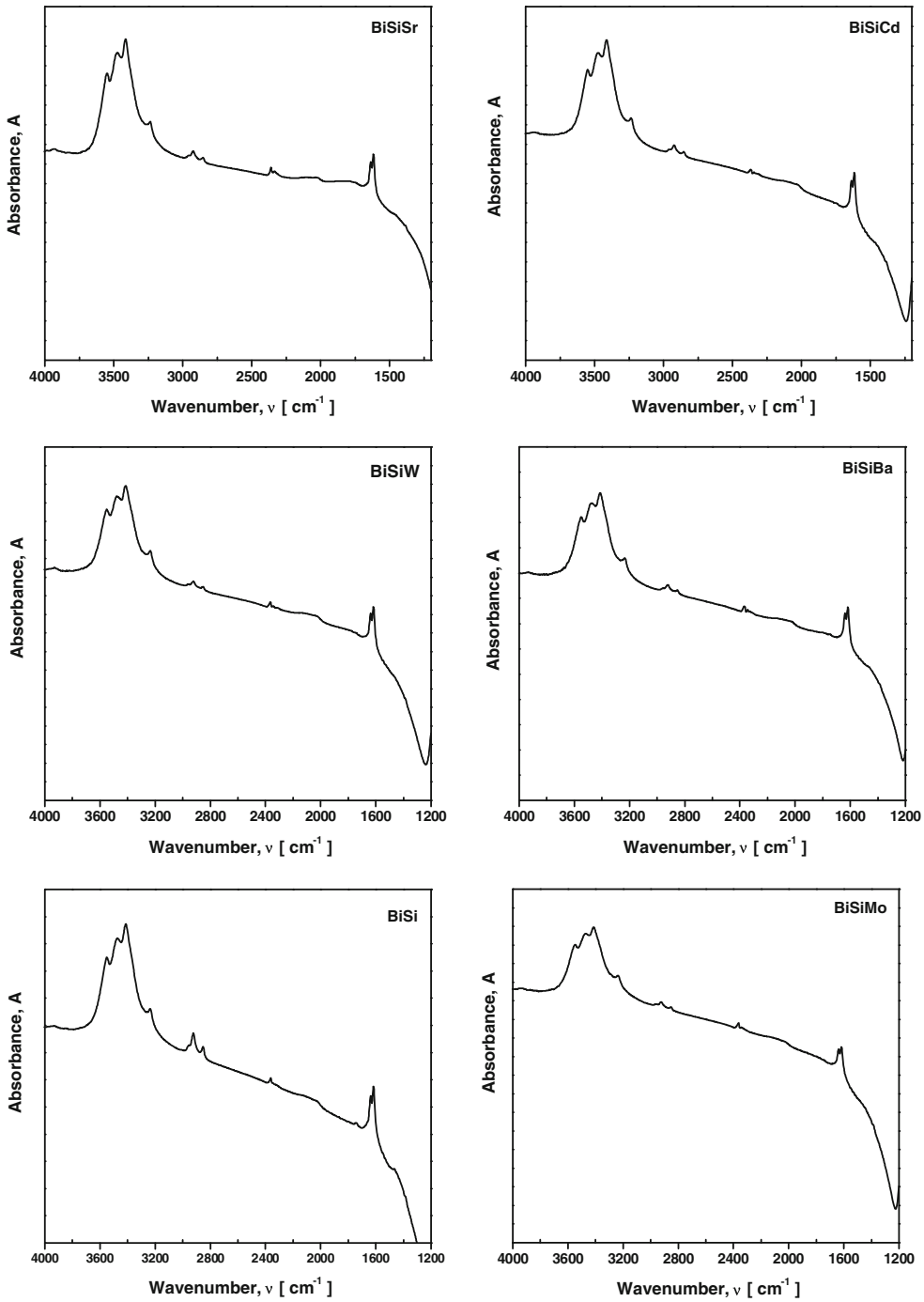

a common structural property; the randomly distributed longitudinal particles are clearly observed through all samples. The parent bismuth silicate (BiSi) glass-ceramic shows besides the elongated particles another few particles having rounded or rectangular structure. Hence, the SEM confirms the existence of two phases in the BiSi glass-ceramic.

For the BiSiMo sample, the elongated particles exist in an amorphous matrix. According to the X-ray diffraction pattern of BiSiMo, the S-Q of the crystals or particles is 68 %, hence the remaining ratio will be expected to be 32 % which can represent the amorphous or the vitreous phase. The S-Q ratio is observed to increase as the molecular weight of the dopant increases to 75 % as in the case of BiSiW, and then the longitudinal particles are condensed and increased as seen in Fig. 3.

It is worth mentioning that BiSiSr shows two phases at the right and the left sides of the figure. The right side represents the elongated crystals, while the left side shows

small spherical particles arranged and aligned like elongated crystals. For the BiSiBa sample the particles which have elongated shape are predominant and few shaped particles appear to deposit on the edge the of elongated crystals.

Finally, the BiSiCd sample shows the crystals deposited on the vitreous phase. These crystals are assumed to be randomly distributed and fewer than the crystals observed for other samples.

3.4 Structural Investigation

Figure 4a, illustrates the FTIR spectra of the studied glass-ceramic samples in the wavenumber range 1200 - 400 cm^{-1}, and Fig. 4b, describes the infrared spectra in the range 4000-1200 cm^{-1}. The base bismuth silicate glass-ceramic sample has the characteristic bands and peaks in the range 1200-400 cm^{-1} as follows:

1. The small band in the range 400-442 cm^{-1} has weak peaks at 412 and 428 cm^{-1} which are indications of the characteristic bending vibrations of Si-O-Si units [30] and Bi-O bonds in BiO_6 units [31], respectively.
2. Another small band in the range 442-500 cm^{-1} has peaks 453, 464, and 478 cm^{-1} due to the presence of the Bi-O-Bi vibration of distorted BiO_6 octahedral units [31, 32].
3. Small kinks appearing at 509 and 528 cm^{-1} connected with the shoulder at about 600 cm^{-1} are related to the change of the local symmetry of highly distorted BiO_6 polyhedra [33], while the presence of the shoulder at 600 cm^{-1} may be related to the bending vibration of O-Si-O modes [34].
4. A weak broad band is exists in the range 675-768 cm^{-1} having a peak at 731 cm^{-1} indicating the presence of symmetric vibrations of Si-O-Si units [34, 35].
5. A medium broad band from 750-1200 cm^{-1} is related to the asymmetric vibration of Si-O-Si modes [34, 35].

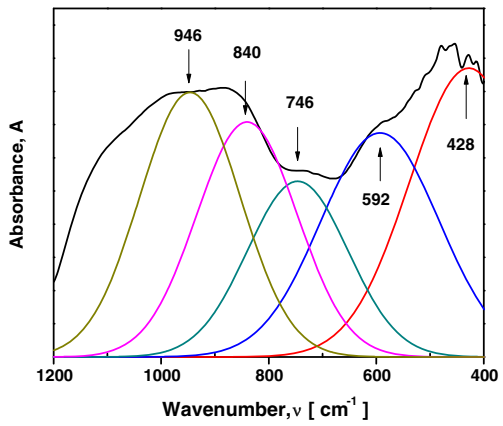

Fig. 5 Deconvoluted peaks for the base bismuth silicate glass-ceramics

On the other hand, the second region from 1200-4000 cm^{-1} for the base bismuth silicate glass-ceramic has the following peaks:

1. The presence of a shoulder at 1460 cm^{-1} may be related to the presence of carbonate groups [35].
2. The strong peak observed at 1622 cm^{-1} is due to the vibrations of water molecules [27].
3. A small peak at about 2362 cm^{-1} and two connected peaks at about 2852 and 2925 cm^{-1} are related to asymmetric and symmetric stretching modes of interstitial H_2O molecules [35, 36].
4. The presence of the broad band from 3000-4000 cm^{-1} comprising peaks at 3240, 3411, 3482, and 3538 cm^{-1} is due to water molecules and the stretching modes of silanol Si(OH) groups [35].

The other glass-ceramic doped samples show nearly the same spectral features with some limited variations in the intensities and the positions of some peaks as clearly observed in Fig. 4a and b.

Hence, there is no indication of the presence of BiO_3 units in the spectral infrared absorption curve. This is unlikely given to the presence of bismuth oxide content in high ratio (65 mol%), so the deconvolution process for the base bismuth silicate infrared absorption spectrum should be obtained in order to detect the vibrational bands of BiO_3 units as a network former besides SiO_4 units. Figure 5 shows the deconvoluted peaks for the base bismuth silicate glass-ceramic sample. As clearly seen from Fig. 5, the presented peaks in the range 1200-400 cm^{-1} can be analyzed into several deconvoluted peaks. The peaks at about 428 and 592 cm^{-1} are described previously as the Bi-O-Bi vibration of BiO_6 octahedral units [31]. Now, symmetric stretching vibration of the Bi-O bonds in BiO_3 units can be detected at 746, 840 and 946 cm^{-1} [31, 32, 37]. It can be deduced that there is overlapping between bands of BiO_n where n = 3 or 46 and SiO_4 units in the spectral range 1200-400 cm^{-1}.

4 Conclusion

The presence of one of different dopants like MoO_3, WO_3, BaO, SrO, or CdO is shown to play the key role in modifying the constitution and properties of bismuth silicate glasses. When bismuth silicate glass is crystallized through thermal heat treatment regimes, eulytite phase is formed through the presence of heavy transition metal oxides like MoO_3, or WO_3. Moreover, samples which were doped with WO_3 are shown to have a good eulytite crystallinity phase. Different phases can be detected with other dopants like bismuth silicate and bismuth oxide silicate phases. Bismuth

oxide silicate ($Bi_2O_2SiO_3$) phase is the main phase of bismuth silicate glass modified with CdO. SEM images reveal that all the samples have elongated shaped particles with some other rectangular or spherical particles. The high ratio of bismuth oxide content is assumed to be mainly acting as a network modifier within SiO_4 network units.

References

1. Sugimito N (2002) Ultrafast optical switches and wavelength division multiplexing (WDM) amplifiers based on bismuth oxide glasses. J Am Ceram Soc 85:1083–1088
2. Pan A, Ghosh A (2000) A new family of lead–bismuthate glass with a large transmitting window. J Non-Cryst Solids 271:157–161
3. Simon V, Todea M, Takàcs AF, Neumann M, Simon S (2007) XPS Study on silica–bismuthate glasses and glass ceramics. Solid State Commun 141:42–47
4. Sun H, Wen L, Xu S, Dai S, Hu L, Jiang Z (2005) Novel lithium–barium–lead–bismuth glasses. Mater Lett 59:959–962
5. Golis E, Kityk IV, Wasylak J, Kasperczyk J (1996) Nonlinear optical properties of lead-bismuth-gallium glasses. Mater Res Bull 31:1057–1065
6. Pan Z, Henderson DO, Morgan SH (1994) Vibrational spectra of bismuth silicate glasses and hydrogen-induced reduction effects. J Non-Cryst Solids 171:134–140
7. Fu J (1995) Formation and properties of glasses in the systems Bi_2O_3-PbO-(ZnF_2, CdF_2). Mater Lett 24:207–210
8. Abdelghany AM (2010) The elusory role of low level doping transition metal in lead silicate glass. Silicon 2:179–184
9. Karthikeyan B, Mohan S (2003) Structural, optical and glass transition studies on Nd^3+- doped lead bismuth borate glasses. Phys B Condens Matter 334:298–302
10. Witkowska A, Rybicki J, Cicco AD (2005) Structure of partially reduced bismuth–silicate glasses: EXAFS and MD study. J Alloys Comp 401:135–144
11. Bale S, Rahman S, Awasthi AM, Sathe V (2008) Role of Bi_2O_3 content on physical, optical and vibrational studies in Bi_2O_3–ZnO–B_2O_3 glasses. J Alloys Comp 460:699–703
12. Holland W, Beall G (2002) Glass–Ceramic Technology american ceramic society. OH, Westerville
13. (2005). In: Shelby JE (ed) Introduction to glass science and technology, 2^{nd} edition The Royal Society of Chemistry. Cambridge, UK
14. Rocha MVJ, Carvalho HWP, Lacerda LCT, Simões G, de Souza GGB, Ramalho TC (2014) Ionic desorption in PMMA–gamma-Fe_2O_3 hybrid materials induced by fast electrons: An experimental and theoretical investigation. Sperctrochimica Acta A 117:276–283
15. Blank TA, Eksperiandova LP, Belikov KN (2016) Recent trends of ceramic humidity sensors development: a review. Sens Actuators B 228:416–442
16. ElBatal FH, Abdelghany AM, ElBatal HA (2014) Characterization by combined optical and FT infrared spectra of 3d-transition metal ions doped-bismuth silicate glasses and effects of gamma irradiation. Spectrochim Acta A 122:461–468
17. Gerth K, Rüssel C (1999) Crystallization of Bi_3TiNbO_9 from glasses in the system Bi_2O_3/TiO_2/Nb_2O_5/B_2O_3/SiO_2. J Non-Cryst Solids 243:52–60
18. Abo-Naf SM, Elwan RL, Elkomy GM (2012) Crystallization of bismuth oxide nano-crystallites in a SiO_2–PbO–Bi_2O_3 glass matrix. J Non-Cryst Solids 358:964–968
19. Takahashi Y, Benino Y, Fujiwara T, Komatsu T (2001) Second harmonic generation in transparent surface crystallized glasses with stillwellite-type $LaBGeO_5$. J Appl Phys 89:5282–5287
20. Murugan GS, Varma KBR, Takahashi Y, Komatsu T (2001) Nonlinear-optic and ferroelectric behavior of lithium borate–strontium bismuth tantalate glass–ceramic composite. Appl Phys Lett 78:4019–4021
21. Takahashi Y, Benino Y, Fujiwara T, Komatsu T (2004) Large second-order optical nonlinearities of fresnoite-type crystals in transparent surface-crystallized glasses. J Appl Phys 95:3503–3508
22. Sambasiva Rao MV, Rajyasree Ch, Narendrudu T, Suresh S, Suneel Kumar A, Veeraiah N, Krishna Rao D (2015) Physical and spectroscopic properties of multi-component Na_2O–PbO–Bi_2O3–SiO_2 glass ceramics with Cr_2O_3 as nucleating agent. Opt Mater 47:315–322
23. Fu F, Chen B, Shen L, Pun EYB, Lin H (2014) Multi-channel transition emissions of Sm^3+ in lithium yttrium aluminum silicate glasses and derived opalescent glass ceramics. J Alloys Comp 582:265–272
24. Tian C, Chen X, Shuibao Y (2015) Concentration dependence of spectroscopic properties and energy transfer analysis in Nd^3+ doped bismuth silicate glasses. Solid State Sci 48:171–176
25. Cheng Y, Xiao H, Guo W (2006) Structure and crystallization kinetics of Bi_2O_3–B_2O_3 glasses. Thermochim Acta 444:173–178
26. Ihara R, Honma T, Fujiwara Y, Komatsu T (2004) Second-order optical nonlinearities of metastable $BiBO_3$ phases in crystallized glasses. Opt Mater 27:403–408
27. Khalil EMA, Elbatal FH, Hamdy YM, Zidan HM, Aziz MS, Abdelghany AM (2010) Infrared absorption spectra of transition metals-doped soda lime silica glasses. Phys B 405:1294–1300
28. Abdelghany AM (2010) The elusory role of low level doping transition metals in lead silicate glasses. Silicon 2:179–184
29. Hammad AH, Marzouk MA, ElBatal HA (2016) The Effects of Bi_2O_3 on Optical, FTIR and Thermal Properties of SrO-B_2O_3 Glasses. Silicon 8:123–131
30. Fuss T, Mogus -Milankovic A, Ray CS, Lesher CE, Youngman R, Day DE (2006) Ex situ XRD, TEM, IR, Raman and NMR spectroscopy of crystallization of lithium disilicate glass at high pressure. J Non-cryst Solids 352:4101–4111
31. Vinaya Teja PM, Ramesh Babu A, Srinivasa Rao P, Vijay R, Krishna Rao D (2013) Structural changes in the ZnF_2–Bi_2O_3–GeO_2 glass system doped with Fe_2O_3 by spectroscopic and dielectric investigations. J Phys Chem Solids 74:963–970
32. Singh K (1997) Electrical conductivity of Li_2O-B_2O_3-Bi_2O_3: a mixed conductor. Solid State Ionics 93:147–158
33. Dimitriev Y, Mihallova V (1992) Proc. Int. Congress on Glass, Madrid. In: Dufan A, Navarro F (eds), vol 3, p 293
34. Elbatal HA, Mandouh ZS, Zayed HA, Marzouk SY, Elkomy GM, Hosny A (2012) Thermal, structure and morphological properties of lithium disilicate glasses doped with copper oxide and their glass–ceramic derivatives. J Non-Cryst Solids 358:1806–1813
35. Elbatal HA, Mandouh Z, Zayed H, Marzouk SY, Elkomy G, Hosny A (2010) Gamma ray interactions with undoped and CuO-doped lithium disilicate glasses. Phys B Condens Matter 405:4755–4762
36. Khalil EMA, ElBatal FH, Hamdy YM, Zidan HM, Aziz MS, Abdelghany AM (2010) Infrared absorption spectra of transition metals-doped soda lime silica glasses. Phys B Condens Matter 405:1294–1300
37. Saritha D, Markandeya Y, Salagram M, Vithal M, Singh AK, Bhikshamaiah G (2008) Effect of Bi_2O_3 on physical, optical and structural studies of ZnO–Bi_2O_3–B_2O_3 glasses. J Non-Cryst Solids 354:5573–5579